Advances in 3D Printing for Electrochemical Energy Storage Systems

Ankitha Menon[1], Abdullah Khan[2], Neethu T.M. Balakrishnan[1], Prasanth Raghavan[1,3], Carlos A. Leon y Leon[2], Haris Ali Khan[4], M.J. Jabeen Fatima[1,*] and Peter Samora Owuor[2,*]

[1]*Materials Science and Nano Engineering Lab, Department of Polymer Science and Rubber Technology, Cochin University of Science and Technology, Kerala, 682022, India*

[2] *Carbon Science Centre of Excellence, Morgan Advanced Materials, State College, Pennsylvania, 16803, USA*

[3]*Department of Materials Engineering and Convergence Technology, Gyeongsang National University, 501 Jinju-daero, Jinju 52828, Republic of Korea*

[4]*Department of Aerospace Engineering, National University of Science and Technology (NUST), H-12, Islamabad, 44000, Pakistan*

Abstract: In the current scenario, energy generation is relied on the portable gadgets with more efficiency paving a way for new versatile and smart techniques for device fabrication. 3D printing is one of the most adaptable fabrication techniques based on designed architecture. The fabrication of 3D printed energy storage devices minimizes the manual labor enhancing the perfection of fabrication and reducing the risk of hazards. The perfection in fabrication technique enhances the performance of the device. The idea has been built upon by industry as well as academic research to print a variety of battery components such as cathode, anode, separator, etc. The main attraction of 3D printing is its cost-efficiency. There are tremendous savings in not having to manufacture battery cells separately and then assemble them into modules. This review highlights recent and important advances made in 3D printing of energy storage devices. The present review explains the common 3D printing techniques that have been used for the printing of electrode materials, separators, battery casings, etc. Also highlights the challenges present in the technique during the energy storage device fabrication in order to overcome the same to develop the process of 3D printing of the batteries to have comparable performance to, or even better performance than, conventional batteries.

Keywords: 3D Printing, Batteries, Electrodes, Separators, Battery casings.

1. INTRODUCTION

The invention of additive manufacturing, popularly known as 3D printing, aimed at achieving two goals: reducing production time and circumventing the many constraints of conventional production methods. It was envisioned that 3D printing could lead to the production of complex geometry parts, interlocking parts that don't need assembly, and single objects in a fast-paced fashion and at a low cost. 3D printing also eliminates the need for tooling and a dedicated production line and hence is beneficial for cost savings in conventional production processes. Faster innovation and mechanization, as well as on-demand customization, can be achieved by 3D printing. An important part of 3D printing was also thought to be a solution to material loss that contributes greatly to final production cost. There is wide interest in using 3D printing in many industries. In this report, we will restrict ourselves to the application of 3D printing in the field of electrochemical devices. Many areas in energy storage have seen an expansion using 3D printing, including electrodes, electrolytes, separators, etc. [1]. This technique is used more often because it can allow for fast prototyping at a relatively low cost. There is a variety of 3D printing techniques currently in use for the above-mentioned applications, namely: fused deposition modeling (FDM), stereolithography (SLA), inkjet printing, direct ink writing, binder jetting, etc. In this introductory part, we will discuss the basic operating principles of a few 3D techniques that we think can be ideal for electrochemical devices.

1.1. Inkjet Printing

Inkjet printing is a droplet-based deposition method that can allow complex patterns with high resolution to be printed. This technique is also suitable for multi-materials printing. It is adaptable to a wide range of materials, such as liquids, suspended solids, and conductive as well as insulating additives. An advantage of inkjet printing compared to other methods is that no post-processing of the finished printed product is needed. It is a low-temperature, low-

*Address correspondence to this author at the Materials Science and Nano Engineering Lab, Department of Polymer Science and Rubber Technology, Cochin University of Science and Technology, Kerala, 682022, India; Tel: +91-(0)-790-7533273, +1-(0)-703-6297114;
E-mail: jabeen@cusat.ac.in; samorapeter@gmail.com

E-ISSN: 2410-4701/21

pressure method involving the deposition of solid suspensions or liquid materials. The printing material is extruded through nozzles or a single nozzle in a print head (see Figure **1a**). The print head raster scans over the surface as layers are built up in a typical layer-by-layer process and cured between successive depositions. Deposited layers are very thin; therefore, fast curing is achieved through low temperature or exposure to infrared or ultraviolet light. The resolution of the printing is mainly controlled by the nozzle sizes. Smaller nozzle sizes tend to achieve very high resolution as they deposit small-size droplets of inks. Inkjet printing has been used to print black phosphorous resulting in stable optoelectronic and photonic devices [2]. It has also been used to print piezoelectric devices [3]. Stable lab-on-chip electrodes have been printed using this technique for incorporation into integrated electrochemical biosensors [4].

1.2. Direct-Ink Writing (DIW)

Direct-Ink Writing (DIW) like FDM is an extrusion-based additive process. The liquid-phase or paste-like ink is dispensed from small nozzles under controlled flow rates. The ink must possess a shear-thinning behavior, high storage modulus, and yield strength that allow shape retention of extruded lines. The deposition is done along a digitally defined path resulting in 3D objects in a layer-by-layer fashion (see Figure **1b**). The produced parts are normally fragile and may need drying, debinding, and sintering to impart desired mechanical properties. DIW is very versatile and can allow a high loading of materials; therefore, it has been used to fabricate supercapacitors, batteries, etc. DIW is less cumbersome to operate than inkjet printing since there is no risk of nozzle clogging. Also, high mass loading of active materials can be loaded that may promote high energy density and areal capacitance [1]. Direct-ink printing has shown to be an effective method to print MXene-based inks for micro-supercapacitors [5]. It was shown that it is possible to synthesize the inks in the absence of any additive or binary solvent systems. Interconnecting electrodes have been achieved using this technique [6]. Modification of the ink can overcome its high surface tension, thereby allowing for the printing of flexible circuits on paper [7].

1.3. Stereolithography (SLA)

Stereolithography (SLA) was the first 3D printing technology patented, back in 1986 [8]. In SLA, a part or object is created in a selective polymer curing or crosslinking process with the aid of an ultraviolet laser beam (see Figure **1c**). The starting materials must therefore be photosensitive thermoset polymers that may come in liquid form with or without additives. SLA is the most cost-effective technique among various 3D printing technologies and can lead to high accuracy and smooth surfaces. SLA can be divided into four processes. (I)The build platform is positioned in the tank containing a liquid photopolymer thermoset a one-layer height distance for the surface of the photopolymer. (II) Ultraviolet (UV) laser beam then creates the next layer by selectively curing and solidifying the photopolymer resin. It is crucial to focus the laser beam in a predetermined path using a set of mirrors (galvos). Scanning is done on the whole cross-sectional area of the model to produce a fully crosslinked solid part. (III) Once a layer is done, the platform moves to a safe distance to let the sweeper blade re-coat the surface. The process then will repeat itself until the whole part is complete. (IV) When printing is finished, the part is fully cured and if further crosslinking is needed for high mechanical properties, post-processing can be done either in UV or with a combination of UV and temperature. The liquid thermoset resin solidifies through photopolymerization. In this solidification process, the resin monomers are activated by light from the UV beam to start a polymerization reaction (mostly by addition polymerization) to form strong chemical bonds.

1.4. Fused Deposition Modeling (FDM)

Fused deposition modeling (FDM) belongs to the material extrusion family of 3D printing. An object or part is built by depositing melted material in a pre-determined path through a layer-by-layer process (see Figure **1d**). The process is synonymous with thermoplastic polymer filament deposition. FDM is the most widely used 3D printing technology employed today, representing the largest installed 3D printers globally. FDM works by melting and depositing thermoplastic polymers by varying the melting temperature of the polymers. The first stage is to load the filament into the printer. Then the nozzle is set to the recommended extrusion temperature of the polymer. The extrusion head is normally able to move in a 3-axis system that is important to allow modeling in X, Y, and Z directions. Extrusion is done in thin strands of the polymer which are deposited layer-by-layer in predetermined locations where the polymer solidifies. Solidification can be accelerated by cooling fans that blow cold air as extrusion progresses. Multiple passes are needed to build a structure to the final required

size. Fused deposition modeling (FDM) is a promising technique for the direct incorporation of the battery in the final 3D object. This can be shown by SiO_2/PLA and lithium iron phosphate/polylactic acid (LFP/PLA) synthesized filaments for printing battery separator and positive electrode components, respectively [9]. The addition of a plasticizer leads to high loading of active materials – as high as 52 wt. % while retaining reasonable flexibility of the filament. In the next sections, we will discuss the 3D printing of battery components such as electrodes, electrolytes, packaging casing, and solid-state batteries.

2. 3D PRINTED ELECTRODES AND THEIR PROPERTIES

The performance of electrochemical energy storage (EES) devices such as batteries and supercapacitors strongly rely on the fabrication methodology and assembly design of electrodes and electrolytes. The geometrical parameters and the architectural built of electrodes and solid-state electrolytes are the controlling factors affecting the device performance, hence limiting the use of traditional fabrication techniques over 3D printing [1]. For the last two decades, 3D printing technology has been emerging as an innovative technique to produce energy storage devices from nano to microscale with high precision and accuracy in geometrical morphology, porosity control, and dimensional tolerances. 3D printed structures not only result in high specific energy and power densities due to integrated material functionalities with multiple additives, but also save time and huge capital cost on post-machining processes. There is no doubt that 3D printing represents a promising approach for the fabrication of next-generation EES devices with enhanced performance due to the well-controlled creation of functionalities at selected surfaces with three-dimensional architectures [11]. The environmental impacts of 3D printing technology have been

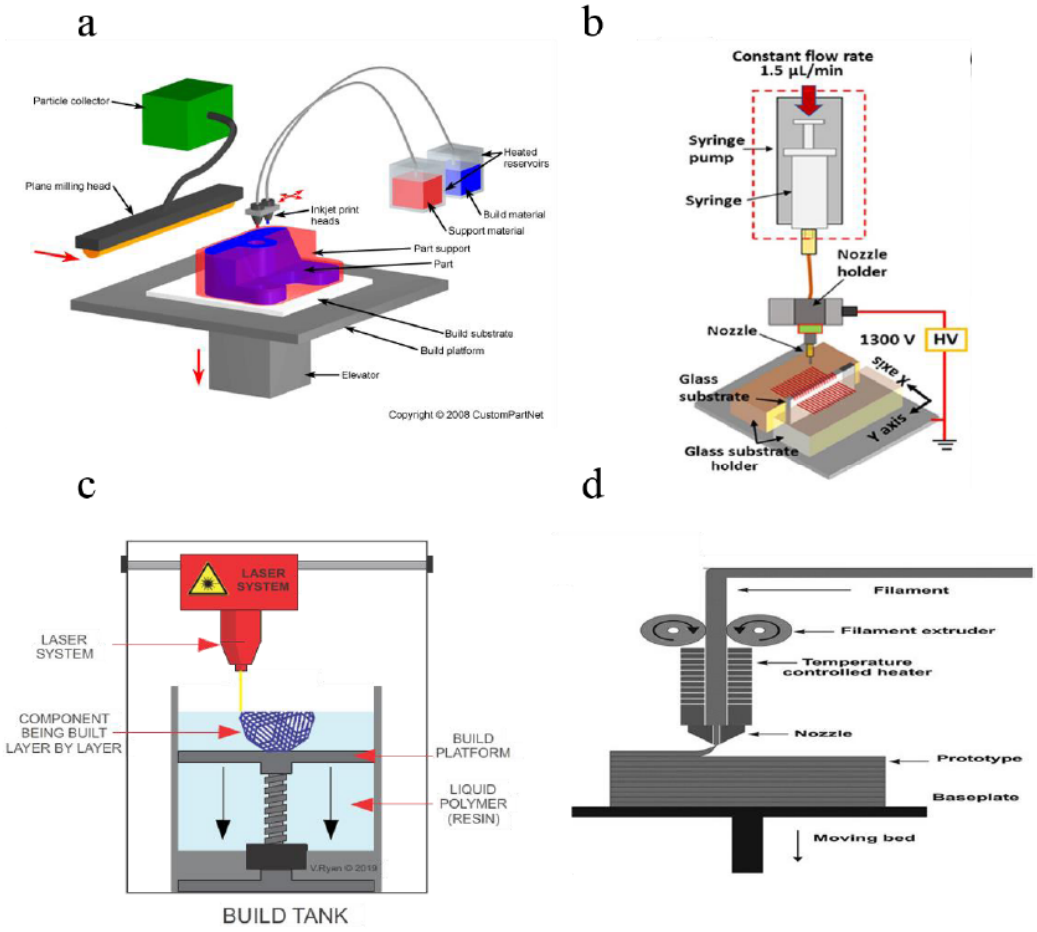

Figure 1: Commonly utilized 3D printing techniques: (**a**) inkjet printing, reprinted with permission from Custom Part Net; (**b**) direct-ink writing; (**c**) stereolithography; and (**d**) fused deposition modeling (FDM), reprinted from ref [10] under Creative Commons License.

investigated both in the US [12] and the EU [13]. The most important aspects of such studies include product life cycle and cost estimation, energy consumption, waste materials, and their recycling, carbon footprints, and air and water pollution. For instance, the US developed an energy assessment model which helps to rank manufacturing processes based on energy consumption. However, in the EU, the focus has been towards efficient utilization of resources and production with zero waste. In fact, 3D printing technology has been reported to be an environmentally friendly solution by providing a clean and healthy environment, and with improved energy efficiency [14, 15]. Electrode fabrication includes top-down and bottom-up approaches as described in Figure **2** [16]. At laboratory and industrial scales, conventional or traditional electrode fabrication methods differ. The most widely used techniques in the research areas are based on various physical/chemical deposition methods such as spray coatings, electrochemical/electrophoretic deposition, physical/chemical vapor deposition, sol-gel synthesis, spin-coatings, atomic layer deposition, and layer-by-layer deposition. However, in industry, high-speed roll-to-roll processing [17, 18] is used to make energy storage devices. This method consists of multiple steps including chemical deposition, electrode rolling, cutting, making a cell assembly with separator, filling the electrolyte, and packaging [1].

In the past few years, multiple 3D printing techniques have been used to manufacture energy storage devices, including inkjet printing [11, 19], direct ink writing [20, 21], binder jet method [22], fused deposition modeling process [23], stereolithography or optical fabrication or photo-solidification or resin printing [24], and metal 3D printing [26]. A technical comparison of the most selected 3D printing techniques for the fabrication of EES devices has been provided in Table **1**.

With the increasing demand for energy storage devices, batteries and capacitors have received a lot of attention in the past few decades. Due to the massive development work in autonomous vehicles, electric cars, and mobile applications, storage of renewable energies is the main focus to improve battery materials, including electrodes with higher capacity, the higher voltage at the positive electrode, longer cycle life,

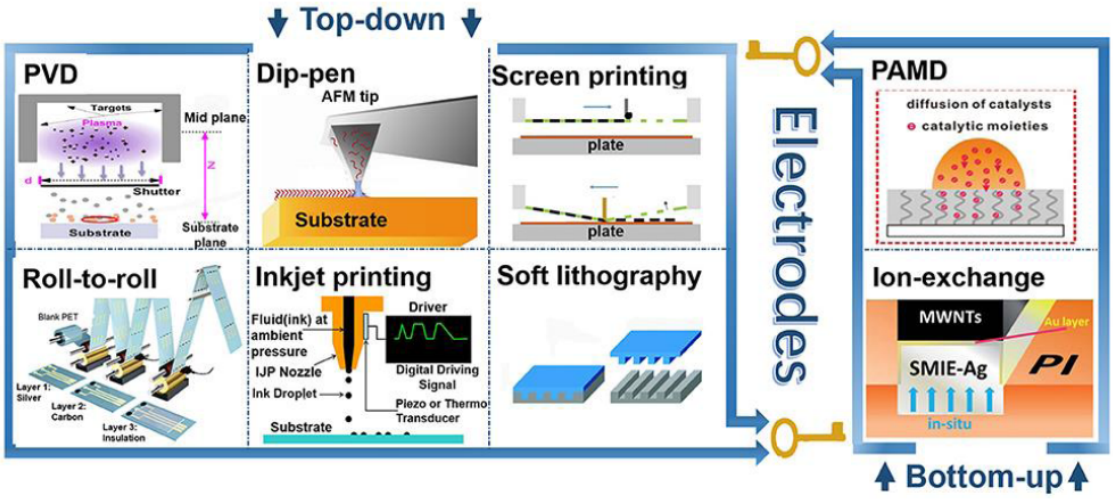

Figure 2: The available technologies for electrode fabrication, including two categories based on the manufacturing process: top-down and bottom-up. Reproduced from ref [16] under Creative Commons License.

Table 1: A technical Comparison of Most Common 3D Printing Techniques used for Making EES Devices [27]

3D Printing Method	Printing Materials	Accuracy	Printing Speed	Cost
Direct ink writing (DIW)	Ceramics, Polymers, Gels	High	High	Low
Fused deposition modeling (FDM)	Ceramics (Some), Photocurable Materials	Low	High	Low
Stereolithography (SLA)	Thermoplastic Polymers	Very high	Low	High
Selective laser sintering (SLS)	Metals, Ceramics, Polymers	High	High	Very high

electrolyte safety, and cost-effective active materials. In the following sections, a few recent developments on 3D printing of electrode materials have been documented.

2.1. Anode Materials

In recent work [28], the electrochemical behavior of ink-jet printed porous composite lithiated iron phosphate-$LiFePO_4$ electrode (positive electrode or anode) from aqueous suspension (wet process) for application in lithium micro-batteries have been investigated. $LiFePO_4$ electrode is coated with 3 wt.% conductive carbon black. The study found that inkjets prepared in aqueous media along with carboxymethyl cellulose standard binder provide more suitable rheological properties with enhanced binding and dispersion as compared to using the low molecular weight poly-acrylic-co-maleic acid copolymer. The electrochemical tests of 3D printed electrodes have been conducted in Swagelok® cells with organic solvent $LiPF_6$/ethylene carbonate-dimethyl carbonate (LP30) or ionic liquid (Li-TFSI- trifluoromethane sulfonylimide salt in propylpyrrolidinium-PYR13-TFSI solution) based electrolyte and lithium foil as the negative electrode. The 3D inkjet-printed thin and porous electrode exhibited very high rate charge/discharge behavior, as well as excellent cyclability, in selected electrolytes-. In the case of LP30 at respective cycling current rates (C) of 9 and 90, very high cell performance of 80 $mAh.g^{-1}$ to 70 $mAh.g^{-1}$ was obtained, which correspond to 36 $\mu Ah.cm^{-2}$ to 32 $\mu Ah.cm^{-2}$, respectively. In addition, at a current rate (C) of 90, a low polarization under only 100 mV was obtained and at a current rate (C) of 9, there was no loss capacity after 100 cycles. Also, at the same current rate and with the ionic liquid-based electrolyte, discharge capacities of 63 $mAh.g^{-1}$, that is 26 $\mu Ah.cm^{-2}$, were obtained.

Graphene/MnO_2 electrodes have been fabricated via 3D printing using the direct ink writing technique [29]. The schematics of the fabrication process have been illustrated in Figure **3** where all the manufacturing steps are explained in a flow diagram. The starting ink mixture composition includes a graphene oxide (GO) suspension (40 mg/mL) and 5% hydroxypropyl methylcellulose. Using this ink, 3D printing was done and just after that, the 3D printed structures were immersed in liquid nitrogen. A GO aerogel was formed by freeze-drying in a vacuum for two days. This step was necessary to maintain the structure without cracks which happen often due to uncontrolled water evaporation and drying out of the structure. These 3D-printed aerogel samples were further heat-treated in a tube furnace under a nitrogen environment at 1050 °C for 3 hours and slowly cooled with a ramp rate of 2 °C/min to convert GO to G aerogel.

MnO_2 nanosheets were coated on 3D printed G aerogel structures by the electrodeposition method. A three-electrode-based electrolytic cell was used for this

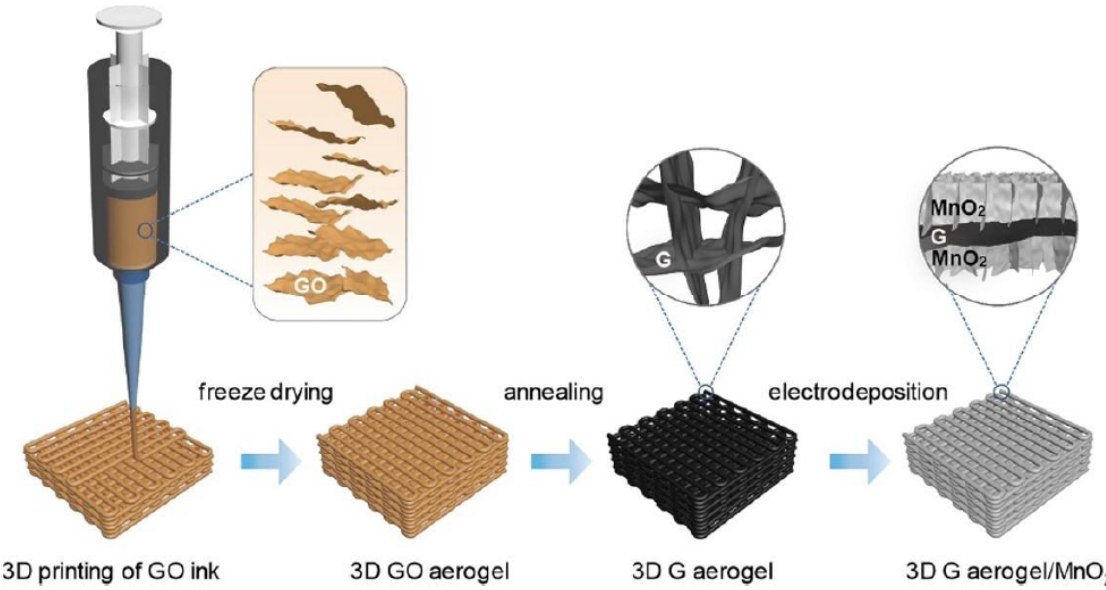

Figure 3: A schematic diagram representing the fabrication process of a 3D Printed Graphene (G) Aerogel/MnO_2 electrode. Printed from ref [29] under Creative Commons License.

purpose where the working electrode, counter electrode, and reference electrode were G aerogel, graphite foil, and saturated calomel electrode (SCE), respectively. The electrolytic cell was operating under a constant current density of 10 mA cm^{-2} with 0.1 M manganese acetate aqueous electrolyte solution. Before coating MnO_2, the thickness of 3D printed G aerogel was 1 mm. By varying the deposition time from 300 to 7200 s, MnO_2 mass loading was varied from 2 to 45.2 mg cm^{-2}. To achieve 2, 3, and 4 mm of MnO_2 coating thickness, the deposition time increased to 14,400, 21,600, and 28,800 s, respectively. The microanalysis of 3D printed electrodes has been presented in Figure **4**.

For the baseline, different substrates including non-3D printed reference or control samples were coated with the comparative amount of MnO_2 using an electrodeposition technique under a similar current density. Substrate materials included carbon paper, carbon fiber, carbon cloth/foil, and non-3D printed graphene aerogel (prepared with a similar process but without employing 3D printing). The electrochemical performance of 3D G electrodes with and without manganese oxide (MnO_2) shas been presented in Figure **5**. Current collectors with MnO_2 deposition showed excellent gravimetric capacitances approaching the theoretical limits. Active material loading, in this case, was below 1 mg cm^{-2}. However, higher mass loading of active materials most often slows down the ion diffusion in bulk material, resulting in a decay of capacitive performance.

Moreover, in this study it was demonstrated that the electrochemical performance of 3D printed graphene aerogel with high MnO_2 loading (182.2 mg cm^{-2}) shows an outstanding areal capacitance of 44.13 F cm^{-2} as illustrated in Figure **6**. It is important to mention that these 3D printed electrodes at the same time can achieve outstanding capacitance if normalized on the

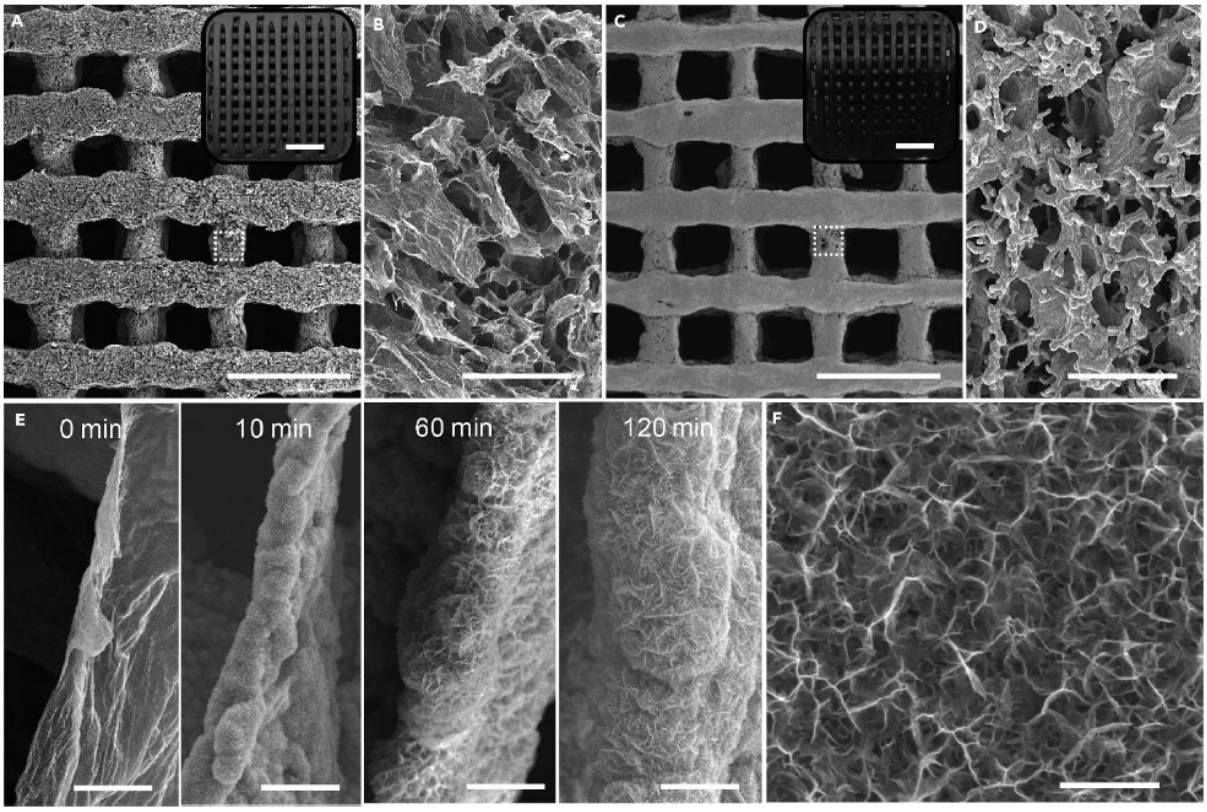

Figure 4: Microanalysis (SEM) of 3D Printed Electrodes. **(A)** 3D printed graphene aerogel lattice (top-view). Scale bar, 1 mm. **(B)** Cylindrical rod highlighted in (**A**) at high magnification. Scale bar, 40 μm. **(C)** 3D printed graphene aerogel lattice electrodeposited with MnO_2 for 600 s (top-view). Scale bar, 1 mm. **(D)** Cylindrical rod highlighted in (**C**) at high magnification. Scale bar, 40 μm. Images shown in insets of (**A**) and (**C**) are 3D printed graphene aerogel and graphene aerogel/MnO_2, respectively (top-view). Scale bars, 5 mm (insets). **(E)** Edge of a graphene nanosheet at different stages of electrodeposition of MnO_2. Scale bars, 2 μm. **(F)** MnO_2 nanosheets electrodeposited on a graphene nanosheet. Scale bar, 300 nm. Printed from ref [29] under Creative Commons License.

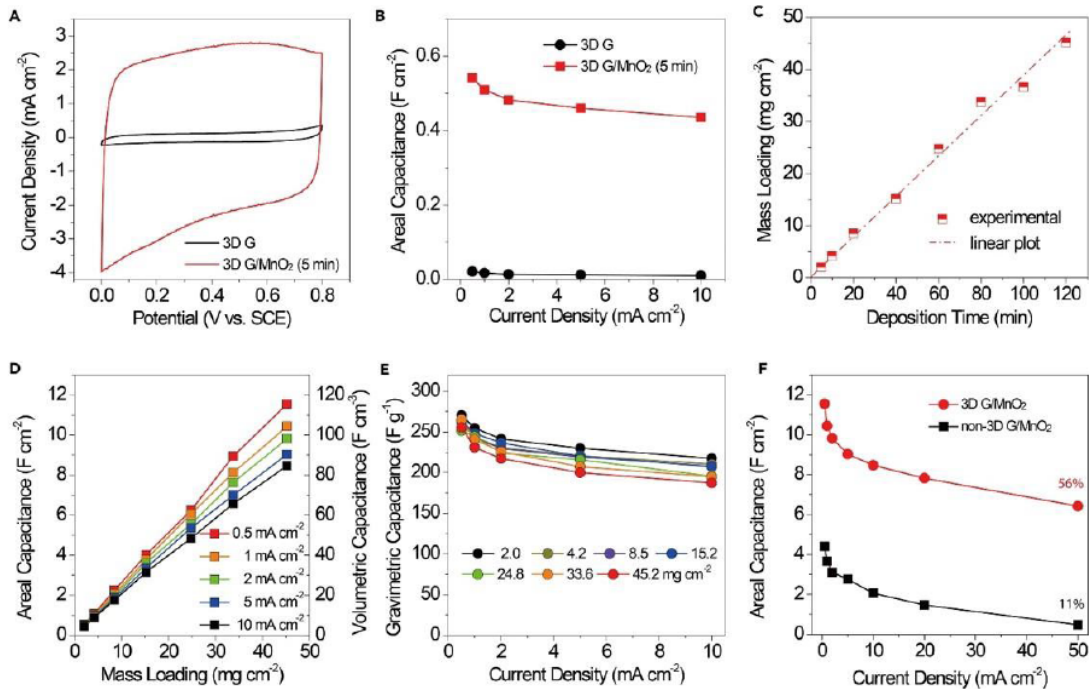

Figure 5: Electrochemical characterization of 3D printed G/MnO_2 Electrodes. **(A)** Typical CV curves of 3D printed G and 3D printed G/MnO_2 electrodes (after 5 min deposition) collected at scan rate of 5 mV/s. **(B)** The areal capacitance of 3D printed G and 3D printed G/MnO_2 electrodes (after 5 min deposition) observed at different current densities. **(C)** The mass loading of MnO_2 versus the electrodeposition time. **(D)** Areal and volumetric capacitances observed for 3D printed G/MnO_2 electrodes with different mass loading of MnO_2 at different current densities. **(E)** Gravimetric capacitances obtained at different current densities from 3D printed G/MnO_2 electrodes with different amounts of MnO_2 loadings. **(F)** At different current densities, the areal capacitances of 3D printed G/MnO_2 and non-3D printed G/MnO_2 electrodes. The percentage values are the capacitance retention percentages when the current density increases from 0.5 to 50 mA cm^{-2}. Printed from ref [29] under Creative Commons License.

surface area, volume, or weight basis, which is not the case for other electrodes.

Another similar study on MoS_2-reduced graphene oxide (rGO) hybrid aerogels for sodium-ion battery anodes has recently been reported [46]. In this work, microstructure and macro-porosity have been controlled via the 3D freeze printing method which is a combination of injecting printing and freeze casting. For inject printing, ink was prepared in aqueous media by mixing ammonium thiomolybdate (MoS_2 precursor) and graphene oxide. A hybrid structure of MoS_2 nanoparticles anchored on the surface of 2D rGO nanosheets in a macroporous framework was achieved by freeze-drying and thermal annealing in a reducing atmosphere. The study reports a remarkably high initial specific capacity over 429 mAh/g at a current rate of 3.3 (C) in the potential range of 2.5–0.10 V (vs. Na^+/Na).

2.2. Cathode Materials

The energy capacity of the cathode materials is equally important to that of anode materials due to the high areal energy and power density requirements for energy storage systems used in transportation and stationary applications. Again for lithium-ion battery applications, new hybrid 3D structure negative electrodes via extrusion-based 3D printing of $LiMn_2O_4$ (LMO) paste were fabricated [47]. The goals were to obtain a higher aspect ratio of electrodes as well as to achieve high loading of active material. The advantages of this manufacturing technique were not limited to the using of the conventional battery paste material by eliminating the solvent preparation required for a typical 3D printing process, which is quite complicated. The new hybrid innovative design and fabrication process also helps to form an interdigitated configuration allowing the existing laminated structure and 3D structure to stick to each other and infuse together. As a result, the battery exhibits excellent performance in both areal and specific capacity. Also, this hybrid design solved the assembly issues arising in building CR2032 battery cells due to the simple and easy assembly process of both laminated and 3D structures. In the cell configuration, cathode and anode materials were LMO and Li foil, respectively. For the

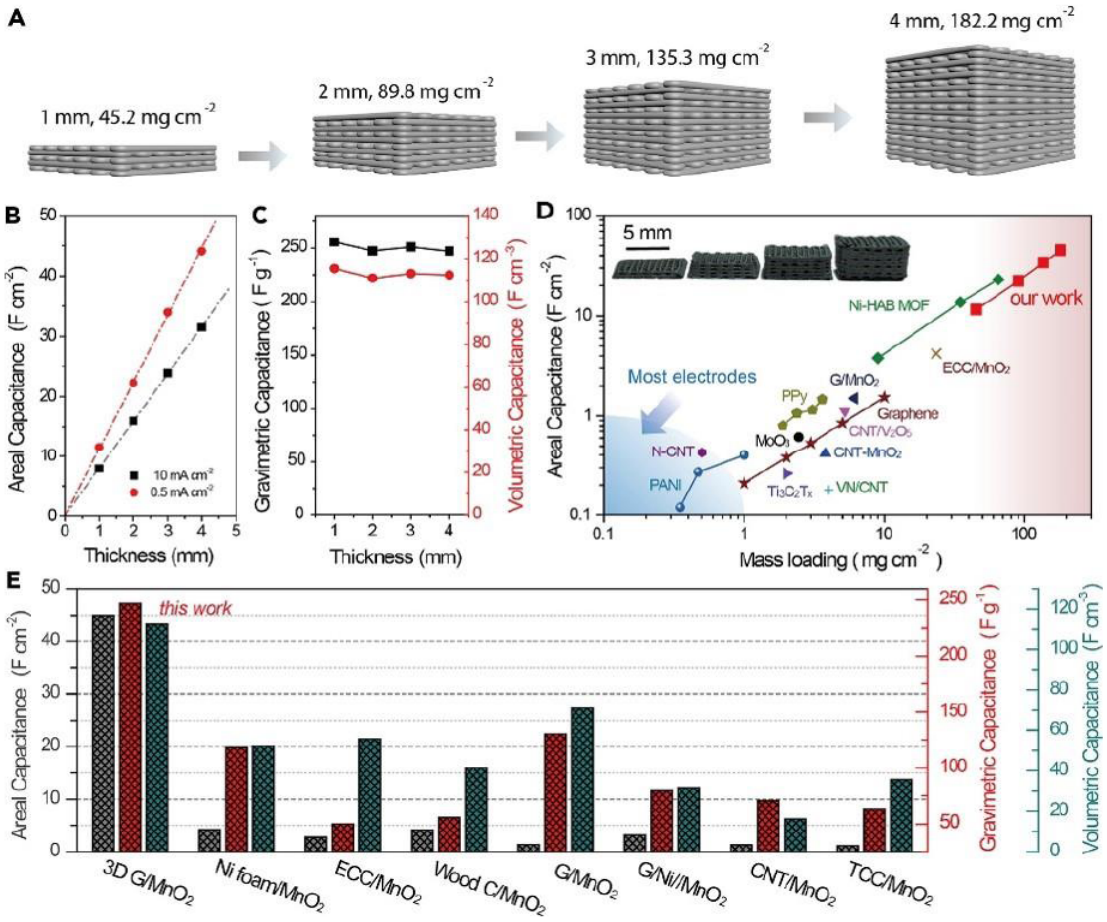

Figure 6: Electrochemical Performance of various thickness (1–4 mm) 3D Printed Graphene/MnO_2 Electrodes. **(A)** Schematic diagram of 3D printed G/MnO_2 electrodes with varying thicknesses and MnO_2 mass loadings. **(B)** The areal capacitance at 0.5 and 10 mA cm^{-2} as a function of electrode thickness. **(C)** Gravimetric and volumetric capacitances as a function of electrode thickness. **(D)** Comparative areal capacitances of 3D printed G/MnO_2 electrodes with the values found in literature (PANI, [30] N-CNT, [31] MoO_3, [32] Ppy [33] Graphene, [34] G/MnO_2, [35] $Ti_3C_2T_x$, [36] VN/CNT, [37] CNT-MnO_2, CNT/V_2O_5, [38] ECC/MnO_2, [39] and Ni-HAB MOF [40]). Inset image: 3D printed G/MnO_2 electrodes with different thicknesses (1–4 mm). **(E)** A comparison between the areal, gravimetric, and volumetric capacitance of the 4-mm-thick 3D printed G/MnO_2 electrode with the literature values reported for MnO_2-based electrodes with high mass loading (Ni foam/MnO_2, [41] ECC/MnO_2, [39] wood C/MnO_2, [42] G/MnO_2, [43] G/Ni/MnO_2, [35] CNT/MnO_2, [44] and TCC/MnO_2 [45]).

separator, commercial polymeric materials PP/PE/PP from Celgard® were used. 1.0 M $LiPF_6$ in EC/DMC=50/50 (v/v), battery grade, was used as liquid electrolyte. Battery performance in terms of specific and areal capacities was analyzed in conventional laminated setup as well as compared with the hybrid system as a function of cathode thickness. In the conventional laminated structure case, the maximum value of specific capacity was 110 ± 5 mAh g^{-1} at 160 µm and then was reduced with an increase in thickness. However, in the hybrid system, the specific capacity was 117 ± 6 mAh g^{-1} even at a higher thickness of 370 µm. Areal capacities of laminated and hybrid structures were 3.5 ± 0.08 mAh cm^{-2} at 370 µm and 4.5 ± 0.3 mAh cm^{-2} at 270 µm, respectively.

In another study [48], the direct ink writing method was used to fabricate both cathode $LiFePO_4$ (LFP) and anode $Li_4Ti_5O_{12}$ (LTO) materials for lithium-ion micro-batteries applications. Using this 3D printing technique, it became possible to fabricate electrodes with a high aspect ratio (wall thickness ~60 µm and height ~200-400 µm) and interdigitated configuration for both LFP and LTO electrodes. These were printed onto a glass substrate patterned with gold current collectors. The performance of these lithium micro-batteries (total volume < 1 mm^3) has been reported as providing an areal capacity of ≈1.5 mAh cm^{-2} during discharge at current rates (C) below 5. Also, LFP electrodes printed with eight layers (~ 200 µm thick) and 16 layers (~ 400 µm thick) delivered the same current density, respectively. However, after 3D printing and

densification, packaging of these lithium micro-batteries by applying hermetic seals is challenging.

In recent work [49], LIBs with LFP as cathode and LTO as anode couple were fabricated using the direct ink writing 3D printing method. This combination is a favored by many researchers due to its excellent thermal stability and low volumetric change upon cycling. These properties are extremely important since they are the main limiting factors for fabricating thick electrodes. In this work, a new generation of 3D printed LIBs with thick, semisolid biphasic electrodes were fabricated by thorough dispersion and mixing of active electrode particles (LFP or LTO), with conductive carbon helping in percolative network formation. The selected ink for the cathode and anode were composed of 30% LFP with 1.25% KB conductive carbon particles and 30% LTO with 1.35% KB conductive carbon particles in 1 m LiTFSI/PC (all by volume %) with 1 wt% polyvinylpyrrolidone PVP% (concerning LFP or LTO), respectively. These rechargeable batteries have exhibited a ten-fold enhancement in areal capacity compared to their previous work [50]. They have reported areal capacities of 4.45 mAh cm^{-2} at 0.14 mA cm^{-2} (≈17.3 Ah L^{-1}), however, corresponding complete cells before packaging can deliver 14.5 mAh cm^{-2} at 0.2 mA cm^{-2} (with an energy density of 20 mWh cm^{-2} at 1 mW cm^{-2}).

Very recently a study was published on fused deposition modeling 3D printing [51], where a composite filament made up of copper/polylactic acid was fabricated via this technique. Subsequent surface functionalization of this filament was done by copper electroplating. The main purpose of this step was to remove the kinetic barrier to electron flow. The electrokinetic properties of the 3D printed electrode with and without surface electroplating were analyzed by cyclic voltammetry using a $[Ru(NH_3)_6]^{3+/2+}$ couple as the electroactive probe. It was found that surface modification by electroplating there was in no kinetic barrier at all. Also, the magnitude of the faradaic response was very much equivalent to those of the conventional metallic and carbon-based electrodes. Moreover, the obtained faradaic peak separation value (70–75 mV) seems superior to all values for 3D printed electrodes reported so far in the literature.

2.3. Properties of 3D Printed Electrode Materials

As noted above, 3D printing approaches to the manufacture of electrodes have recently been recognized as a fast, inexpensive, and environmentally friendly alternative to conventional fabrication methods [51]. Robust electrodes with high performance typically used in specialized electrochemical flow reactors can indeed be fabricate with this technology. As mentioned earlier, electrode materials with geometrically complex structures and controlled porosity or pore size distribution can be produced by additive manufacturing techniques. This is important because it is known that both active surface area and mass transport properties have a big impact on the electrochemical performance of an electrode. Consequently, it is possible to improve battery performance by tailoring the surface of a versatile, free form electrode with 3D printing technology. Moreover, using 3D printing, electrodes with different surface roughness, microstructure, orientation, composition, electrocatalytic properties, and fluid flow environments can conceivably be fabricated.

For the first time, researchers used a powder-bed additive manufacturing technique to fabricate porous 300 mm thick graphene-based electrodes for supercapacitor applications [22]. It was reported that high gravimetric and areal capacitance values of 260 F g^{-1} and 700 mF cm^{-2}, respectively, were achieved for this thick supercapacitor electrode. In this study, the porosity, and microstructures of two electrodes, one fabricated through additive manufacturing and the other mechanically pressed, were compared. It was found that the electrodes developed through additive manufacturing had more porous microstructure compared to its mechanically pressed counterpart. It was also observed that pores were more interconnected, which favors their acting as channels for transporting ions. Moreover, using this additive manufacturing technique palladium nanoparticles were decorated on thermally reduced graphene oxide (TRGO) sheets to decrease the contact resistance at the interface of powder agglomerates. This resulted in an improvement in electronic conduction and consequently, the gravimetric and areal capacitance values were boosted up by a factor of two and seven, respectively. Porous electrode materials have a larger specific surface area as compared to planar electrodes, thereby offering superior space-time yield and more channels for mass transport. These are the reasons why porous electrodes have demonstrated excellent electrochemical performance in redox flow batteries for energy storage and different industrial processes such as catalysis and others. A recent study [52] on highly ordered porous electrodes in electrochemical flow reactors has demonstrated a clear demarcation among

planar versus porous structure. In this work, a stainless-steel structure was produced by 3D printing followed by electrodeposition of nickel coatings from an acidic bath. Linear sweep voltammetry and chronoamperometry methods were used to determine the mass transport kinetics (volumetric mass transport coefficient during electrochemical reduction reaction of 1.0×10^{-3} mol dm^{-3} of ferricyanide ions). To confirm the novelty and the benefits of 3D printed porous electrodes for electrochemical flow reactors, the diffusion kinetics were analyzed and compared with those of other geometries. According to this study, it is possible to use 3D printing to design and produce robust porous electrodes with tailored surface area, compositional features, structured volumetric porosity, and defined mass flow characteristics. The study concluded that mass transport characteristics of a 3D-printed Ni/Stainless-Steel porous electrode are comparatively better than those of typical planar, mesh, and RVC electrodes of the same material.

A very interesting work on structure-property relationship has recently published [53] where polycrystalline micropillars were fabricated by a novel 3D printing method and their behavior was analyzed under compressive loads. Micropillar compression testing is a very common technique to study the mechanical behavior of various engineering materials. The technique involves fabricating micropillars of different polycrystalline materials with a variety of microstructures, sizes, and textures through different processing techniques. For instance, milling using focused ion beam (FIB), nanoimprinting, vapor deposition, and electrodeposition methods are very popular to fabricate micropillars of different engineering materials. However, in this study, a direct 3D printing followed by sintering of nanoparticles was used as a bottom-up fabrication technique to make polycrystalline micropillars with varying microstructures. These micropillars were then tested under compression. Two classes of micropillars were compared. The one with small grain sizes and high porosity pillars showed brittle behavior and higher effective modulus. However, micropillars with larger grain sizes appeared to have low porosity. Moreover, the latter samples were highly ductile and had a lower effective modulus. The unusual trend of effective stiffness reduction with decreasing porosity percentage was linked using a model that captures the combined effects of grain size and porosity and relates the morphology and distribution of pores to their fundamental structure-property relationships. Based on the results of this study, 3D printing fits well under the definition of a novel method for the fabrication of micropillars, since using this approach it became possible to produce varying microstructures from micro- to meso-length scales of polycrystalline materials. We expect that this study will enhance the fundamental understanding of the chemical compatibility, electrochemical deposition, and/or etching relevant to the control of microstructure and orientation of the particles or grains in electrode materials.

3. 3D printed Electrolyte Materials and their Properties

With the advent of Electric Vehicles (EVs) and more focus on renewable energies, a paradigm shift is noted in improving the current performance of commercial , in particular battery Lithium-Ion Batteries (LIBs) [9]. One of the methods for improving battery performance is through increasing their energy density by tailoring their properties. However, properties of the electrolyte, recent researches show that increased energy density is associated with safety hazards. For instance, liquid electrolytes can be flammable, volatile, and prone to form unstable interfaces and electrolyte passivation layers [54]. To mitigate such challenges, solid-state electrolytes emerge as viable candidates which provide more chemical stability, are inherently safer, and can contribute towards maximizing the energy density [55]. Nevertheless, as with liquid electrolytes, there are a few challenges associated with solid-state electrolytes which hinder their exploitation to their maximum potential. One of the major impediments is propagation of lithium dendrites, which can result in short-circuiting and premature battery failure [24]. Researchers demonstrated that this problem can be abridged by applying surface coatings [56]. Another major obstacle for the commercialization of solid-state electrolytes is their relatively high cell Area Specific Resistance (ASR), which arises from poor electrode-electrolyte contact [57, 58], due to high interfacial electrode-electrolyte impedance, where the high impedance values are a result of the low conductivity and long diffusion distances involved. It is thought that solid-state electrolytes are inherently less conformant to the electrolyte surface than the liquid electrolytes, thereby reducing the areal interface. Moreover, most of the advanced solid-state electrolytes are manufactured through a conventional powder metallurgy method, whereby the electrolyte powders are pressed in the form of pellets and further sintered to achieve uniform

density. This mode of manufacturing reduces the geometric contact area to the planar faces. These obstacles can be addressed by placing a highly high-porous electrolyte layer on top of an interfacial layer of the same material [58]. This strategy helps in increasing the contact area through the porous layers, while the thin, interfacial layer provides the shortest ion diffusion path. Looking at these aspects, it is evident that state-of-the-art manufacture of solid-state electrolytes requires novel electrolyte cell designs, while Additive Manufacturing (AM) techniques in general, and 3D printing, can in particular, provide a perfect foil for abridging the gaps in the existing solid-state electrolyte cell design. Owing to the unique advantages of achieving free-form design and tailored properties through previously discussed 3D printing techniques, intricate chemical, structural, mechanical, thermal, and electrical requirements of modern electrolytes can be attained [59].

3.1. Properties of Printed Battery Cases

The function of an electrolyte in a typical energy storage device is to permit the smooth movement of ions between the electrodes. Certain key design and manufacturing requirements are discussed in the preceding paragraphs which can be translated into the desired structural, chemical, mechanical, and electrical properties. Some of those key properties are safety, electrical performance (low activation energy, low electronic conductivity, and high ionic conductivity), cycle life, and chemical stability.

Different 3D printing techniques have been employed to date for the printing of electrolytes using different organic and composite materials to improve electrochemical and mechanical performance of battery electrodes. For instance, researchers in Ref. [60] have employed a novel stencil printing process followed by ultraviolet (UV) curing to print solid-state composite electrolyte (SCE) layer and SCE matrix-embedded electrodes on complex geometries to obtain a multi-layered battery. Through improving the rheological properties of the electrolyte, improved electrochemical performance as compared to that of conventional batteries was demonstrated. In another study, the same printing procedure has been adopted to produce an inflammable and flexible gel electrolyte (*i.e.*, sebaconitrile (SBN)-based electrolyte and a semi-interpenetrating polymer network (semi-IPN) skeleton) which was further used as a principal element to print solid-state gel composite electrolytes [61]. Through a series of experimental tests, the authors have demonstrated improved electrochemical performance, thermal and mechanical stability owing to the inherent flexibility and inflammable nature of the electrolytes as compared with the traditional organic carbonate-based electrolyte. More importantly, this printing procedure has eradicated the need for high pressure/high-temperature sintering required by traditional solid-state preparation processes. In yet another research study, Cheng *et al*. [62] improved the structural integrity of the battery by directly printing a solid poly (vinylidene fluoride-hexafluoropropylene) (PVDF-HFP) on MNO_2 cathode. This scheme increased the adhesion by forming a dense layer, thereby reducing the chance of short-circuiting. McOwen and his co-workers [63] have demonstrated the superior use of garnet-type lithium lanthanum zirconia (LLZ) through developing multiple solid inks of the material using direct ink writing (DIW). The developed varieties of ink formulations have demonstrated favorable microstructure and lower ASR values, thereby improving the conductivity. Multi-stage stereolithography (SL) was employed by Zekoll *et al*. [64] to achieve 85% porosity which resulted in improved conductivity and mechanical properties. Chen *et al*. [65] developed a UV-curable poly (ethylene glycol)-based resin by SL printing a 3D gel polymer electrolyte for micro-LIBs. The authors demonstrated an improved ionic conductivity like that of liquid electrolytes at room temperature.

Other key aspects towards electrolyte selection are their long-term cyclability, suppressed dendrite formation (for added safety), and high-rate capability which can be achieved through well-controlled porosity [66]. However, traditional techniques limit the ability to control pore sizes to develop high-performance electrolytes. A novel 3D printing method was proposed by Blake *et al*. to provide control over the porosity [67]. For this purpose, the authors developed ceramic–polymer electrolytes using glycerol and PVDF which were dissolved in NMP and later mixed with Al_2O_3. Upon drying, the controlled porous microstructure was observed due to the separation of glycerol and PVDF. Excellent thermal stability and improved cycle life compared to those of at the traditional electrolyte (Celgard 2325) were observed for the designed ceramic–polymer electrolyte.

To conclude, it can be inferred that different 3D printing techniques have been employed to date to solve the issues related to solid-state electrolytes manufactured through conventional techniques. A

summary of the key processes, materials used, and desired properties are presented in Table **2**.

3.2. Applications

The application of the 3D printed electrolytes can be expanded to different products and industries. For instance, multidimensional/multiscale complex-structured power sources can greatly benefit if different 3D printing techniques such as fine-precision inkjet or stereolithography are combined to obtain optimized electrolyte topology and architecture. In a similar vein, the ease of design, form, and throughput provided by the 3D printed electrolytes enables their use in smart grids. Furthermore, soft portable electronic devices, which include wearable sensors, flexible batteries, medical implants, and radio-frequency identification tags, can reach their next technology readiness level if the 3D electrolytes are incorporated in their architecture. In effect, the bending, folding, and transparency of energy storage devices and sensors are directly related to the quality of the electrolyte materials and their fabrication methods. Similarly, the prospects and feasibility of manufacturing solid-state energy devices through 3D printing techniques have shown encouraging signs to overcome the technical barriers and improve the compatibility of solid-solid interfaces.

3.3. Future Directions

Although the literature suggests that active research is being performed on the 3D printing of electrolytes, some additional research directions need to be extensively pursued. Firstly, the need for new electrochemically active materials is overarching. Currently, limited printable materials are available, which mostly involve inorganic materials. Since the inks should possess appropriate surface tension, density, and dynamic viscosity, in this regard, a multidisciplinary approach is required which includes manufacturing, material science, surface chemistry, and mechanical engineering domains. Secondly, more experimental, and computational studies are required which can explain the process-structure-property relationships involved. On a similar note, ion transport energy studies to understand the effect of printed electrolyte geometry/structure on ion transfer from the electrolyte-electrode interface are still in their infancy. Extensive studies are required for topology optimization of the 3D printed electrolytes. Moreover, the avoidance of liquids and solvents is likely to drive future designs of commercial energy storage devices (batteries, capacitors, etc.) towards solid-state electrolyte systems. This will in turn open new opportunities in 3D printing materials and methods suitable for solid electrolyte manufacture.

4. 3D PRINTED BATTERY CASES

Battery cases are the structural covering provided to protect the components from external stimuli, thus enhancing the safety of the batteries. These structural blocks consist of grooves or channels to hold the electrodes intact. The casing material also demands high thermal and chemical stability. The desirable properties of archetypal battery cases or covers depend on the battery for which the cases or covers

Table 2: Process-Material-Property Mapping for 3D Printed Electrolytes

Process	Material	Targeted Property
Stencil printing	a) Solid-state composite b) Sebaconitrile (SBN)-based electrolyte	a) Low activation energy b) High conductivity c) Thermal and mechanical stability.
Direct Ink Writing	Poly vinylidene fluoride-hexafluoropropylene) (PVdF-HFP)	Long cycle time
Direct Ink Writing	Lithium lanthanum zirconia (LLZ)	High ionic conductivity
The dry phase inversion method	Ceramic-polymer	a) Thermal stability b) Mechanical stability c) Improved electromechanical performance
Stereolithography	a) Bi-continuous Li1:4Al0:4Ge1:6$(PO_4)_3$ (LAGP) ceramic electrolyte b) Ceramic polymer electrolyte	a) Ionic conductivity b) Mechanical properties c) Improved cycle life d) Thermal stability

are designed. The electrochemical batteries can be broadly divided based on the electrochemistry and stability of the components incorporated in the device. The conventional lead-acid batteries involve non-flammable components whereas the ion-type batteries involve flammable components like lithium, and therefore the components employed will also vary accordingly. The ingredients and development of the batteries selectively focuses on the structure and constituents of the cases. Strength, rigidity, inertness, tunability, low cost, etc., are some of the major properties under consideration for battery cases.

Based on their performance and function, the battery cases can be classified as non-conducting battery cases or conducting battery cases. In miniature batteries like coin cells, AA or AAA batteries, etc., the cases are composed of metal and are conducting. Most of these metal coatings are comprised of stainless steel. But as the size of the batteries (modules) increases, the packaging systems will be focused on inert, rigid, and thermally insulative materials which mostly comprise polymers. A schematic illustration of the classification of battery cases based on materials employed to make the cases has been depicted in Figure **7**.

4.1. Selected 3D Printed Methods for Battery Cases

The methods employed for the fabrication of battery cases can also be broadly classified based on the materials used for their manufacture. The methods are uncommon for commercial purposes and are still in the stage of infancy in the division of battery cases. According to the requirements of the battery cases, the methods for the manufacture of battery cases can be divided into (a) metal 3D printing, and (b) plastics 3D printing. The 3D printers for metals are very sophisticated instruments. The precursors of these printers are usually metallic powders. These metal powders are then fused in the required texture using these instruments to form the design. The first patent of a 3D printer for fusing powder to build 3D structures was developed by Prof. Emanuel M. Sachs of Massachusetts Institute of Technology, Cambridge, who patented a new binder jetting process in 1989 that emerged as the basis of the binder jetting model of 3D printers for metals [68]. Nowadays 3D printers for metal deposition can be divided into two major categories: binder jetting, and powder bed fusion.

The process of binder jet technology utilizes metal powder for deposition. The process includes the usage of a liquid binding material that adheres the powder together to build up the required structure. The sophisticated instruments also contain specialized parts to remove the excess non-bonded particles from the building structures. The binder jet technique was used for the manufacture of a stainless steel (316) battery cases. The sintered density and shrinkage of the printed -three-dimensional structures can be varied through the addition of additives like nylon 12, etc., thereby improving the properties of the printed structures [69]. Stainless steel (420) with different porosities was also fabricated by the binder jet technique followed by sintering at elevated temperatures, which resulted in structures with porous interconnected open channels. Subsequent infiltration

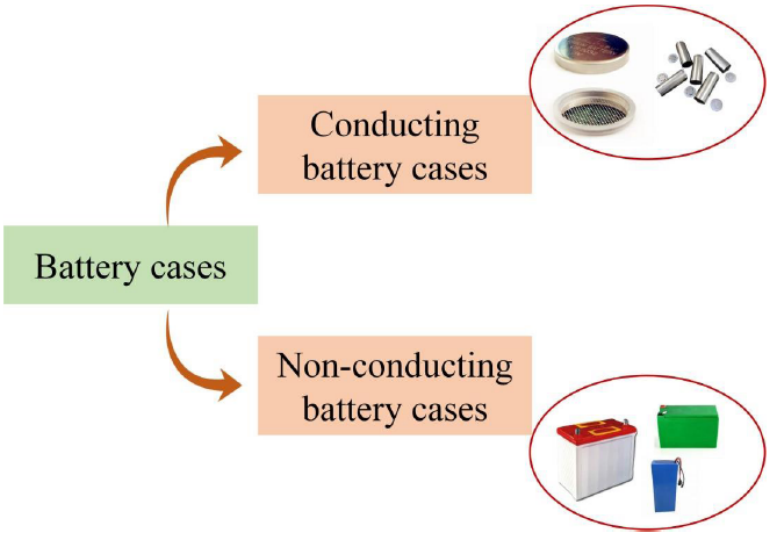

Figure 7: Schematic illustration of the classification of battery cases based on materials used to make them.

with bronze was carried out to enhance the mechanical properties of the material [70]. A relative density of 99.6 % was reported for stainless steel (316L) without infiltration and structural distortion, which was achieved by the selective decomposition of the binder particles enhancing the fusion of the metal imparting the structural rigidity and mechanical strength of the three-dimensional structures [71]. The reports revealed the formation of voids and interconnected channels in the three-dimensional structures owing to the post sintering of the structure to remove the binder particles. The electrochemical energy storage devices strictly require the absence of contact with the ambient atmosphere; hence the method of binder jet technology was found to be an inappropriate technique for the application.

The powder bed fusion technique utilizes the fusion of the powdered metal particles with higher energy laser or electron gun beams to fuse the particles forming firm and rigid structures. The layers are bonded together followed by the spreading of the powder by the powder jet, and then followed by joining to the previous phase. Thus, each layer is manufactured by a step-by-step procedure to form a continuous -three-dimensional rigid structure. Mainly two types of powder bed fusion techniques are commercially available based on the heat sources employed (laser and electron beam). The variants include selective laser sintering (SLS), selective laser melting (SLM) (discussed in the introduction), direct metal laser sintering (DMLS), electron beam melting (EBM), etc.

The fabrication via a laser-based powder bed fusion technique of stainless steel (316L) reveals its superior mechanical properties and wear rate [72]. These structures also showed superior creep ductility compared with similar SS manufactured by conventional methods [73]. Stainless steel (316L) coatings were fabricated on carbon steel substrates (1018) using the powder bed fusion-selective laser melting (PBF-SLM) method. These substrates showed superior corrosion-resistance [74]. Recycled stainless steel powder (AISI 304 L) was also employed for the fabrication of structures using the powder bed fusion technique. The process revealed the advantages of the method as indicated by the formation of superior quality structures [75]. The properties of the stainless steel produced by this method revealed that this fabrication technique is an adequate method for the development of battery cases.

The plastics used for battery cases are mostly fabricated with acrylonitrile butadiene styrene (ABS) and polypropylene (PP). The manufacture of ABS and PP cases via three-dimensional printing can be achieved by fused deposition modeling (discussed earlier). The ABS is considered as be the most prominent material for the fabrication of battery cases. The mechanical strength of pristine ABS was improved by Zhong *et al*. [76] by incorporating short glass fiber, plasticizer, and compatibilizer followed by the modeling. Similarly, the mechanical properties of ABS were improved by incorporation of an organically modified montmorillonite (OMMT), which resulted in an enhancement by almost 50 % of its mechanical properties compared to those of the pristine polymer [77]. Apart from the fillers, the parameters of FDM itself affect the mechanical properties of the ABS structures. Important FDM parameters include the interlayer cooling time (ILCT), nozzle diameter, infill density, raster angle, and layer thickness [78]. The semi-crystalline polypropylene samples have rarely been used for the fabrication of 3D structures. Pertinent studies revealed that FDM parameters such as the extrusion temperature, printing speed, and layer height showed small influence on the mechanical properties of the polymer structures [79]. To summarize, both ABS and PP polymers are appropriate for the fabrication of battery cases by 3D printing.

4.2. Properties of Printed Cases

The primary properties of the battery cases are their chemical and thermal inertness. The materials must be stable in both acidic and alkaline conditions. The components must also have high thermal stability. The stainless-steel cases used for the fabrication of coin cells utilize SS 316L material. The covers of larger battery modules, such as the cases lead-acid batteries, lithium-ion batteries, etc., are fabricated using ABS. The superior chemical and temperature stability and the low cost of ABS makes this material a a more appropriate candidate for the fabrication of cases for large module batteries.

5. 3D PRINTED SOLID-STATE BATTERIES

The recent advancements in 3D printing technologies have given life to the real possibility of manufacturing cheaper batteries with enhanced energy densities that can be customized on customer demand for a wide range of applications. The unique characteristic of using 3D printing technologies for their production is its ability to develop novel designs and thereby enabling the exploration of the possibilities of imparting newer shapes to the batteries. The major

benefits can be categorized into two, viz. the use of batteries as structural components and the tuning of battery shape as per the product design [80].

The pioneering work of 3D printed solid batteries was done at Harvard University in the year 2013 by Jennifer A. Lewis and co-workers [48]. Figure **8** depicts their schematic illustration of a 3D printed micro-battery. They successfully developed lithium-ion batteries which were approximately the size of a grain of sand. Despite this milestone development in the history of batteries, these 3D printed batteries made of special cathode inks and anode were not able to power much. Seven years later two organizations, Blackstone Resources [81] and KeraCel from Switzerland and the US, respectively, announced the successful attempts to create completely 3D printed batteries. The latter company is the receiver of the key patent for its innovation in monolithic solid-state battery technology which incorporates anodes in a sealed manner. Reports suggest that researchers from Singapore and China have developed ways to 3D print flexible batteries for wearable electronics. A thorough literature survey of completely 3D Printed solid-state batteries pointed out that nearly all the research has dedicated to lithium-ion batteries [61, 80, 82].

The digital printing methods categorized under the umbrella of additive manufacturing techniques are fused deposition modeling (FDM), direct ink writing – an extrusion-based process, stereolithography (SLA), selective laser sintering (SLS), and laser-induced forward transfer (LIFT) – with the laser-based processes, aerogel jet printing and ink jetting, based on material jetting methodologies. The capabilities of the mentioned technologies allow the manufacturer to use ceramic or polymeric materials to design and develop completely 3D printed solid-state batteries. The use of additive manufacturing to build and develop large-scale production capabilities for solid-state batteries is at a blooming stage. The initial challenge was to produce 3D printed cathodes with microporous structures. Laser-based technology, and specifically stereolithography, was used for the additive manufacturing of a cathode matrix. This matrix is comprised an intercalated ionic phase with high conductivity embedded within a ceramic material which also imparts electronic conductivity. Recently the technique of aerogel jetting has also been shown to be useful for 3D printing porous scaffolds for lithium-ion batteries. Completion of the design and development of porous cathodes is readily followed by electrolyte deposition. The techniques employed for electrolyte deposition purposes are ink jetting or aerogel jetting.

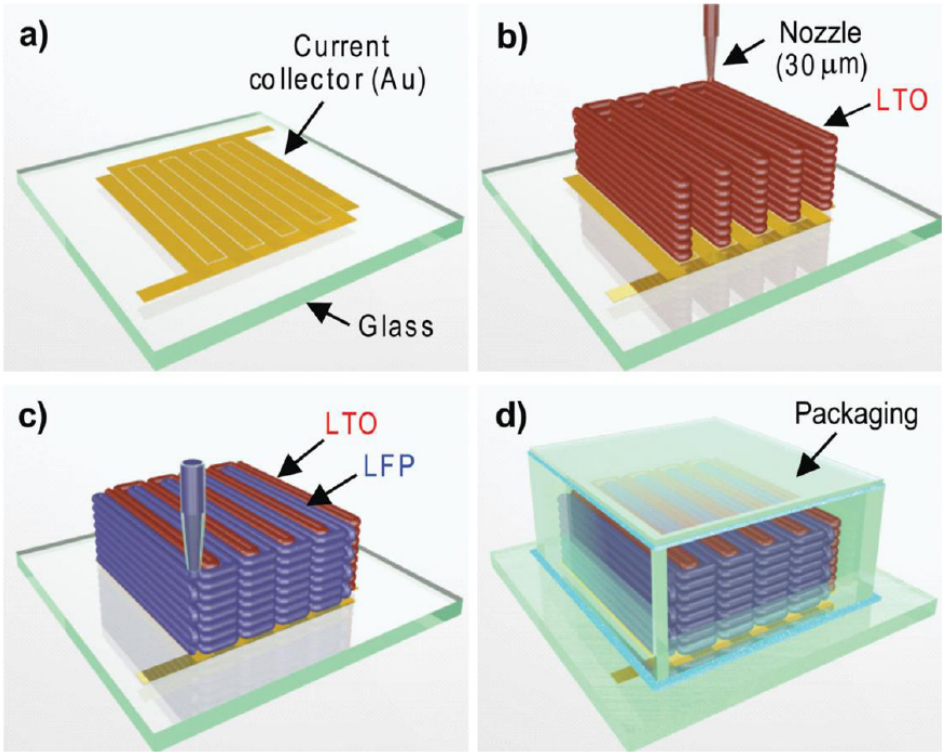

Figure 8: Schematic representation of 3D interdigitated microbattery architectures: (**a**) 3D printed gold current collectors; (**b**) Fused deposition of $Li_4Ti_5O_{12}$ (LTO) and (**c**) $LiFePO_4$ (LFP) inks; and (**d**) Casing. Adapted and reproduced from [48].

These techniques are useful since they allow the infiltration of the solid electrolyte deep into the porous cathodes.

The microporous cathodic material and the bulk electrolyte are required to possess an interface between them. For the deposition of layers with micron-scale dimensions, direct-write techniques or methods of jetting using polymeric, ceramic, or hybrid materials can be used. These methods are also capable of forming high aspect ratio features to promote very high volumetric energy densities. However, the use of direct-write methods was unsatisfactory as the layer thickness of these interfaces could not be controlled at the nanoscale level. Implementation of FDM printing is also advisable in cases where high speeds are required. Despite the high speed that FDM offers, this method also fails to provide adequate control over layer thickness of interfaces beyond a certain limit. Thus, even though the current status of printing technology does not provide nanoscale resolution control of the spatial arrangement of battery components, ink jetting and aerogel jetting at present are the best available options to compete against the conventional thin-film generating techniques like vapor deposition.

3D printing technologies are suitable for the development and manufacture of complex 3D batteries that possess relatively higher surface areas with resolution at the microscopic scale. Any available shape could be modified simply by altering the CAD file with low-cost customization. One clear advantage of using additive manufacturing is the minimal wastage of battery materials [83]. The development of fully 3D printed solid-state batteries by Blackstone indeed set a milestone in the history of lithium-ion batteries. Their research has been geared towards developing batteries that offer greater energy density and a greater number of cycles for charging. As previously mentioned, the major advantages that are being imparted by employing additive manufacturing technologies include a significant reduction in the cost of batteries, an improved the flexibility of the cells, and an increase in energy density of batteries. 3D printing also aids in reducing the fraction of materials that do not store energy, such as copper and aluminum, in batteries [81].

As seen above the most widespread technique employed in 3D printing at present is the fused deposition modeling. The first and foremost work on 3D printing lithium Lithium-ion batteries completely was done by Reyes *et al* [80]. The challenge in developing LIBs by 3D printing is the poor ionic conductivity of filaments that are typically used for FDM printing. Research on efforts to increase the ionic conductivity of the printing filaments reports the use of aluminum oxide, ethylene carbonate, and lithium -perchlorate-based PLA composites [80, 84] (Figure **9**).

Thus, it is possible to use additive manufacture via the FDM method to 3D print batteries with ionic conductivity-enhanced filaments. At the same time, the performance of 3D printed batteries reported in previous research studies were two orders of magnitude behind those of conventional batteries, and that is too low to be used for practical applications. Reports suggest that potential fillers like graphene oxide could be used to activate the presently available filaments. These results could render benefits to those researchers en-route to developing energy storage devices additively.

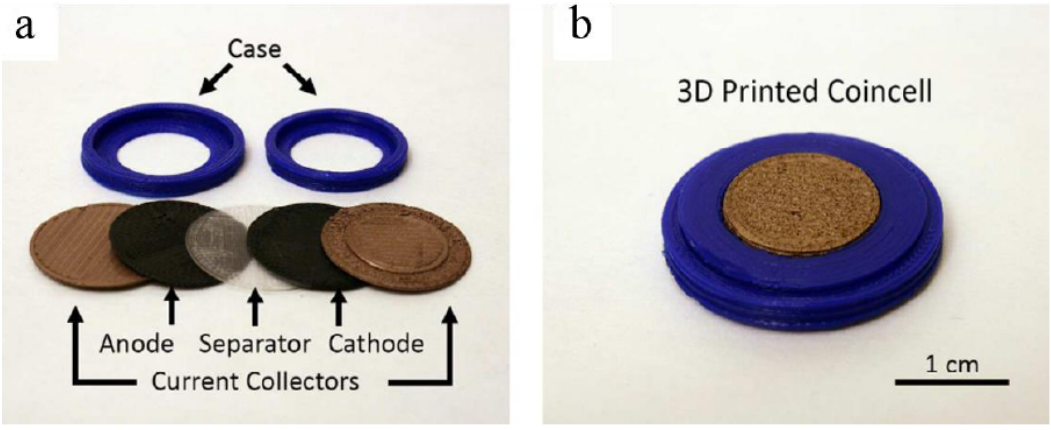

Figure 9: Individual and integrated components of 3D printed coin-cells. Adapted and reproduced from Ref [61].

5.1. Applications of 3D Printed Solid State Batteries

The dawn of 3D printed electronic devices has created a surge in demand and applications of additive manufacturing. To address this demand, Lewis and her co-workers developed a multi-material 3D printer capable of manufacturing electronic devices additively with the aid of Fused Filament Fabrication techniques in combination with ink-jetting [85]. The 3D printing of electronic devices is still clinging around the use of conventional batteries. This restricts the geometrical designs and scales that the products could adopt. As a leaping step towards meeting these challenges, Foster *et al*. tried to 3D print lithium-ion anode disk electrodes for a coin cell with the then available graphene-based filament [80]. The ability to additively manufacture a wide range of shapes and different sizes of batteries as well as their components will enable the use of these 3D printed devices in wearable electronics with a customized shapes and sizes [61, 82]. A recent depiction of such an application was presented by Reyes *et al*. [80] (Figure **10** showcases their product devices) by developing two kinds of electronic devices with 3D printed batteries integrated within them. Each component of the battery was individually printed, followed by infusion with an electrolyte and later by its assembly into the printed cases. The 3D printed batteries were employed to power LCD sunglasses and LED bangles. The latter required curved anodes and cathodes in their batteries, a feature which is difficult to be attained by conventional practices of battery manufacture.

The advent of additive manufacturing could pave the way to mobile usability and unusual shape diversity, including wearable and flexible electronic devices, robotic suits, and sensors [61].

6. SUMMARY AND FUTURE DIRECTIONS

The technology of 3D printing has emerged as a versatile technique for the development of smart materials utilizing the designing software. The advancement in energy storage technology and need for efficient energy storage devices has paved a way to the development of 3D printing of energy storage devices. The commercialization of the fabrication techniques is expected to minimize man power with extreme perfection in the manufacturing process. Nevertheless, although significant progress has been made in 3D printed battery components, there still exist numerous hurdles that need to be solved for making printed batteries with acceptable metrics. The reactive nature of electroactive battery materials needs to be addressed. Also, anodes and cathodes are very complex structural materials which sometimes, for the

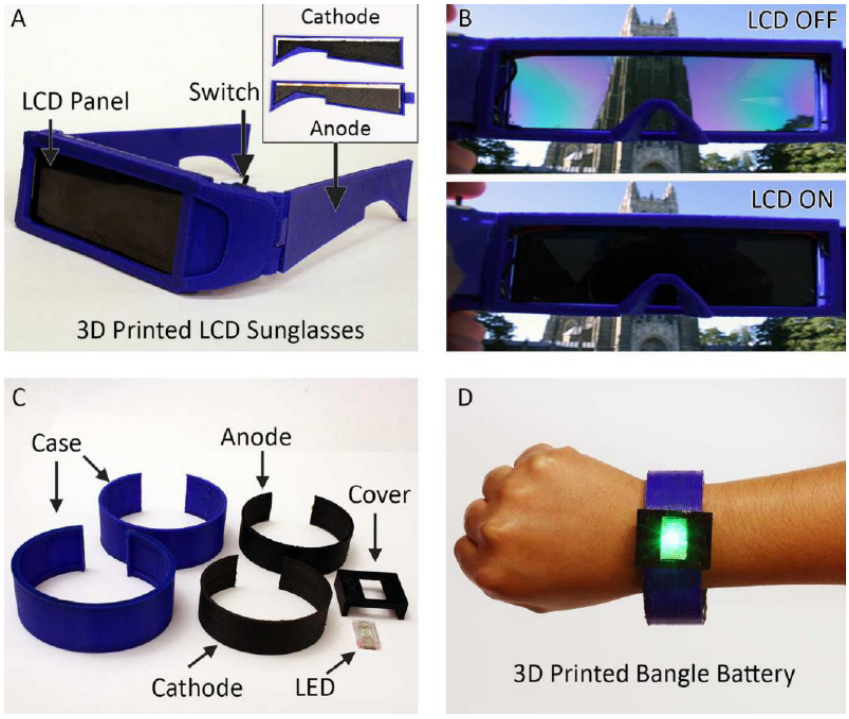

Figure 10: (**A**) 3D printed LCD glasses with integrated 3D printed batteries. (**B**) Demonstration of the LCD in on and off state. (**C**) 3D printed components of a 3D printed bangle battery. (**D**) Assembled 3D printed bangle battery powering an LED. Adapted and reproduced from ref [80].

better performance, may need special ordering like crystals or porous structure akin to molecular sponges. This presents a challenge for 3D printed electrodes. In fact, a major hurdle is still the synthesis of suitable materials for printing. Furthermore, the printed batteries must pass strict safety standards. Despite the above-mentioned problems, we believe there is a strong case for pursuing novel and promising 3D printed batteries.

ACKNOWLEDGEMENT

The authors J.F.M.J, A.M and P.R greatly acknowledge Kerala State Council for Science, Environment and Technology (KSCSTE) and University Grants Commission (UGC) for financial support.

CONFLICTS OF INTERESTS

The authors declare no conflicts of interest.

AUTHOR CONTRIBUTIONS

J.F., A.M., A.K., C.L.L., H.K., and P.S.O. all drafted and compiled sections of the manuscripts. P.S.O. and P.R. edited, proof read, and finalized the manuscript.

REFERENCES

[1] Zhang F. *et al*. 3D printing technologies for electrochemical energy storage. Nano Energy 40, 418-431 (2017). https://doi.org/10.1016/j.nanoen.2017.08.037

[2] Hu G. *et al*. Black phosphorus ink formulation for inkjet printing of optoelectronics and photonics. Nat. Commun. 8, 278 (2017). https://doi.org/10.1038/s41467-017-00358-1

[3] He B, Yang S, Qin Z, Wen B & Zhang C. The roles of wettability and surface tension in droplet formation during inkjet printing. Sci. Rep. 7, 1-7 (2017). https://doi.org/10.1038/s41598-017-12189-7

[4] Papamatthaiou, S. *et al*. Ultra stable, inkjet-printed pseudo reference electrodes for lab-on-chip integrated electrochemical biosensors. Sci. Rep. 10, 1-10 (2020). https://doi.org/10.1038/s41598-020-74340-1

[5] Zhang C. (John) *et al*. Additive-free MXene inks and direct printing of micro-supercapacitors. Nat. Commun. 10, 1-9 (2019). https://doi.org/10.1038/s41467-019-09398-1

[6] Rahman MK. *et al*. Three-dimensional surface printing method for interconnecting electrodes on opposite sides of substrates. Sci. Rep. 10, 1-14 (2020). https://doi.org/10.1038/s41598-020-75556-x

[7] Zheng Y, He Z, Gao Y & Liu J. Direct desktop printed-circuits-on-paper flexible electronics. Sci. Rep. 3, 1-7 (2013). https://doi.org/10.1038/srep01786

[8] Hull CW. Apparatus for production of three-dimensional objects by stereolithography. US Patent US4575330A (1984).

[9] Maurel A. *et al*. Three-dimensional printing of a LiFePO4/Graphite battery cell via fused deposition modeling. Sci. Rep. 9, 1-14 (2019). https://doi.org/10.1038/s41598-019-54518-y

[10] Olivera S, Muralidhara HB & Venkatesh K. Evaluation of surface integrity and strength characteristics of electroplated ABS plastics developed using FDM process. The 17th Asian Pacific Corrosion Control Conference 27-30 (2016).

[11] Zhu C. *et al*. 3D printed functional nanomaterials for electrochemical energy storage. Nano Today 15, 107-120 (2017). https://doi.org/10.1016/j.nantod.2017.06.007

[12] America Makes & AMSC. Standardization roadmap for additive manufacturing - Version 2.0. Am. Makes ANSI Addit. Manuf. Stand. Collab. 2, 1-269 (2018).

[13] Wimpenny D & Holden M. Additive manufacturing aiming towards zero waste and efficient production of high-tech metal products (AMAZE). Amaz. Proj. 74 (2017).

[14] Garg A, Lam JSL & Savalani MM. Laser power based surface characteristics models for 3-D printing process. J. Intell. Manuf. 29, 1191-1202 (2018). https://doi.org/10.1007/s10845-015-1167-9

[15] Khosravani MR & Reinicke T. On the environmental impacts of 3D printing technology. Appl. Mater. Today 20, 100689 (2020). https://doi.org/10.1016/j.apmt.2020.100689

[16] Li Q. *et al*. Review of printed electrodes for flexible devices. Front. Mater. 5, 1-14 (2019). https://doi.org/10.3389/fmats.2018.00077

[17] Stuart BW, Tao X, Gregory D & Assender HE. Roll-to-roll patterning of Al/Cu/Ag electrodes on flexible poly(ethylene terephthalate) by oil masking: a comparison of thermal evaporation and magnetron sputtering. Appl. Surf. Sci. 505, 144294 (2020). https://doi.org/10.1016/j.apsusc.2019.144294

[18] Wood DL. *et al*. Perspectives on the relationship between materials chemistry and roll-to-roll electrode manufacturing for high-energy lithium-ion batteries. Energy Storage Mater. 29, 254-265 (2020). https://doi.org/10.1016/j.ensm.2020.04.036

[19] Giannakou P, Slade RCT & Shkunov M. Cyclic Voltammetry Studies of Inkjet-printed NiO supercapacitors: Effect of substrates, printing and materials. Electrochim. Acta 353, 136539 (2020). https://doi.org/10.1016/j.electacta.2020.136539

[20] Wei M. *et al*. 3D direct writing fabrication of electrodes for electrochemical storage devices. J. Power Sources 354, 134-147 (2017). https://doi.org/10.1016/j.jpowsour.2017.04.042

[21] Feng Y, Li J, Tian R & Yao J. Writing ink-promoted synthesis of electrodes with high energy storage performance: A review. J. Energy Chem. 53, 433-440 (2021). https://doi.org/10.1016/j.jechem.2020.05.031

[22] Azhari A, Marzbanrad E, Yilman D, Toyserkani E & Pope MA. Binder-jet powder-bed additive manufacturing (3D printing) of thick graphene-based electrodes. Carbon N. Y. 119, 257-266 (2017). https://doi.org/10.1016/j.carbon.2017.04.028

[23] Kim H. *et al*. Enhanced dielectric properties of three phase dielectric MWCNTs/BaTiO3/PVdF nanocomposites for energy storage using fused deposition modeling 3D printing. Ceram. Int. 44, 9037-9044 (2018). https://doi.org/10.1016/j.ceramint.2018.02.107

[24] Zeng L. *et al*. Recent progresses of 3D printing technologies for structural energy storage devices. Mater. Today Nano 12, 1-13 (2020). https://doi.org/10.1016/j.mtnano.2020.100094

[25] Wang Y, Chen R & Liu Y. A double mask projection exposure method for stereolithography. Sensors Actuators, A Phys. 314, 112228 (2020). https://doi.org/10.1016/j.sna.2020.112228

[26] Gadagi B & Lekurwale R. A review on advances in 3D metal printing. Mater. Today Proc. 45, 277-283 (2020). https://doi.org/10.1016/j.matpr.2020.10.436

[27] Cheng M, Deivanayagam R & Shahbazian-Yassar R. 3D Printing of Electrochemical Energy Storage Devices: A Review of Printing Techniques and Electrode/Electrolyte Architectures. Batter. Supercaps 3, 130-146 (2020). https://doi.org/10.1002/batt.201900130

[28] Delannoy P. E. *et al*. Ink-jet printed porous composite LiFePO4 electrode from aqueous suspension for microbatteries. J. Power Sources 287, 261-268 (2015). https://doi.org/10.1016/j.jpowsour.2015.04.067

[29] Yao B. *et al*. Efficient 3D Printed Pseudocapacitive Electrodes with Ultrahigh MnO2 Loading. Joule 3, 459-470 (2019). https://doi.org/10.1016/j.joule.2018.09.020

[30] Yao B. *et al*. Paper-based solid-state supercapacitors with pencil-drawing graphite/polyaniline networks hybrid electrodes. Nano Energy 2, 1071-1078 (2013). https://doi.org/10.1016/j.nanoen.2013.09.002

[31] Lin T. *et al*. Nitrogen-doped mesoporous carbon of extraordinary capacitance for electrochemical energy storage Science. 350, 1508-1513 (2021). https://doi.org/10.1126/science.aab3798

[32] Yao B. *et al*. Flexible transparent molybdenum trioxide nanopaper for energy storage. Adv. Mater. 28, 6353-6358 (2016). https://doi.org/10.1002/adma.201600529

[33] Yuan L. *et al*. Polypyrrole-coated paper for flexible solid-state energy storage. Energy Environ. Sci. 6, 470-476 (2013). https://doi.org/10.1039/c2ee23977a

[34] Yang X. *et al*. Liquid-mediated dense integration of liquid-mediated dense integration of graphene materials for compact graphene Materi. 341, 534-537 (2019). https://doi.org/10.1126/science.1239089

[35] Zhai T. *et al*. 3D MnO2-graphene composites with large areal capacitance for high-performance asymmetric supercapacitors. Nanoscale 2013; 5: 6790-6796. https://doi.org/10.1039/c3nr01589k

[36] Ghidiu M, Lukatskaya MR, Zhao MQ, Gogotsi Y & Barsoum MW. Conductive two-dimensional titanium carbide 'clay' with high volumetric capacitance. Nature 516, 78-81 (2015). https://doi.org/10.1038/nature13970

[37] Xiao X. *et al*. Freestanding mesoporous VN/CNT hybrid electrodes for flexible all-solid-state supercapacitors. Adv. Mater. 25, 5091-5097 (2013). https://doi.org/10.1002/adma.201301465

[38] Wu J. *et al*. A Scalable free-standing V2O5/CNT film electrode for supercapacitors with a wide operation voltage (1.6 V) in an aqueous electrolyte. Adv. Funct. Mater. 26, 6114-6120 (2016). https://doi.org/10.1002/adfm.201601811

[39] Song Y. *et al*. Ostwald ripening improves rate capability of high mass loading manganese oxide for supercapacitors. ACS Energy Lett. 2, 1752-1759 (2017). https://doi.org/10.1021/acsenergylett.7b00405

[40] Feng D. *et al*. Robust and conductive two-dimensional metal-organic frameworks with exceptionally high volumetric and areal capacitance. Nat. Energy 3, 30-36 (2018). https://doi.org/10.1038/s41560-017-0044-5

[41] Yang J, Lian L, Ruan H, Xie F & Wei M. Nanostructured porous MnO2 on Ni foam substrate with a high mass loading via a CV electrodeposition route for supercapacitor application. Electrochim. Acta 136, 189-194 (2014). https://doi.org/10.1016/j.electacta.2014.05.074

[42] Chen C. *et al*. All-wood, low tortuosity, aqueous, biodegradable supercapacitors with ultra-high capacitance. Energy Environ. Sci. 10, 538-545 (2017). https://doi.org/10.1039/C6EE03716J

[43] He Y. *et al*. Freestanding three-dimensional graphene/MnO2 composite networks as ultralight and flexible supercapacitor electrodes. ACS Nano 7, 174-82 (2013). https://doi.org/10.1021/nn304833s

[44] Lv P, Feng YY, Li Y & Feng W. Carbon fabric-aligned carbon nanotube/MnO2/conducting polymers ternary composite electrodes with high utilization and mass loading of MnO2 for super-capacitors. J. Power Sources 220, 160-168 (2012). https://doi.org/10.1016/j.jpowsour.2012.07.073

[45] Nakayama M, Osae S, Kaneshige K, Komine K & Abe H. Direct growth of Birnessite-type MnO2 on Treated carbon cloth for a flexible asymmetric supercapacitor with excellent cycling stability. J. Electrochem. Soc. 163, A2340-A2348 (2016). https://doi.org/10.1149/2.1031610jes

[46] Brown E. *et al*. 3D printing of hybrid MoS2 -graphene aerogels as highly porous electrode materials for sodium ion battery anodes. Mater. Des. 170, 107689 (2019). https://doi.org/10.1016/j.matdes.2019.107689

[47] Li J, Leu MC, Panat R & Park J. A hybrid three-dimensionally structured electrode for lithium-ion batteries via 3D printing. Mater. Des. 119, 417-424 (2017). https://doi.org/10.1016/j.matdes.2017.01.088

[48] Sun K. *et al*. 3D printing of interdigitated Li-ion microbattery architectures. Adv. Mater. 25, 4539-4543 (2013). https://doi.org/10.1002/adma.201301036

[49] Wei TS, Ahn BY, Grotto J & Lewis JA. 3D Printing of Customized Li-Ion Batteries with Thick Electrodes. Adv. Mater. 30, 1-7 (2018). https://doi.org/10.1002/adma.201703027

[50] Wei TS. *et al*. Biphasic electrode suspensions for Li-ion semi-solid flow cells with high energy density, fast charge transport, and low-dissipation flow. Adv. Energy Mater. 5, 1500535 (2015). https://doi.org/10.1002/aenm.201500535

[51] Vaněčková E. *et al*. Copper electroplating of 3D printed composite electrodes. J. Electroanal. Chem. 858, 113763 (2020). https://doi.org/10.1016/j.jelechem.2019.113763

[52] Arenas LF, Ponce de León C & Walsh FC. 3D-printed porous electrodes for advanced electrochemical flow reactors: A Ni/stainless steel electrode and its mass transport characteristics. Electrochem. commun. 77, 133-137 (2017). https://doi.org/10.1016/j.elecom.2017.03.009

[53] Sadeq Saleh M, Hamid Vishkasougheh M, Zbib H & Panat R. Polycrystalline micropillars by a novel 3-D printing method and their behavior under compressive loads. Scr. Mater. 149, 144-149 (2018). https://doi.org/10.1016/j.scriptamat.2018.02.027

[54] Qiao Y. *et al*. 3D-Printed Graphene Oxide Framework with Thermal Shock Synthesized Nanoparticles for Li-CO2 Batteries. Adv. Funct. Mater. 28, 1-7 (2018). https://doi.org/10.1002/adfm.201805899

[55] Chen A, Qu C, Shi Y & Shi F. Manufacturing Strategies for Solid Electrolyte in Batteries. Front. Energy Res. 8, 1-18 (2020). https://doi.org/10.3389/fenrg.2020.571440

[56] Luo W. *et al*. Transition from Superlithiophobicity to Superlithiophilicity of Garnet Solid-State Electrolyte. J. Am. Chem. Soc. 138, 12258-12262 (2016). https://doi.org/10.1021/jacs.6b06777

[57] Kotobuki M, Munakata H, Kanamura K, Sato Y & Yoshida T. Compatibility of Li7La3Zr2O12 solid electrolyte to all-solid-state battery using li metal anode. J. Electrochem. Soc. 157, A1076 (2010). https://doi.org/10.1149/1.3474232

[58] van den Broek J, Afyon S & Rupp JLM. Interface-engineered all-solid-state li-ion batteries based on garnet-type fast Li+ conductors. Adv. Energy Mater. 6, 1600736 (2016). https://doi.org/10.1002/aenm.201600736

[59] Khan HA & Ademujimi T. Development of Novel Hybrid Manufacturing Technique for Manufacturing Support

Structures Free Complex Parts. Proceedings of the ASME 2019 14th International Manufacturing Science and Engineering Conference. Volume 1: Additive Manufacturing; Manufacturing Equipment and Systems; Bio and Sustainable Manufacturing. Erie, Pennsylvania, USA. June 10-14, 2019. V001T02A022. ASME. https://doi.org/10.1115/MSEC2019-2928

[60] Kim SH. *et al*. Flexible/shape-versatile, bipolar all-solid-state lithium-ion batteries prepared by multistage printing. Energy Environ. Sci. 11, 321-330 (2018). https://doi.org/10.1039/C7EE01630A

[61] Kim SH. *et al*. Printable solid-state lithium-ion batteries: A new route toward shape-conformable power sources with aesthetic versatility for flexible electronics. Nano Lett. 15, 5168-5177 (2015). https://doi.org/10.1021/acs.nanolett.5b01394

[62] Cheng M. *et al*. Elevated-temperature 3D printing of hybrid solid-state electrolyte for li-ion batteries. Adv. Mater. 30, 1-10 (2018). https://doi.org/10.1002/adma.201800615

[63] McOwen DW. *et al*. 3D-Printing Electrolytes for Solid-State Batteries. Adv. Mater. 30, 1-7 (2018). https://doi.org/10.1002/adma.201707132

[64] Zekoll S. *et al*. Hybrid electrolytes with 3D bicontinuous ordered ceramic and polymer microchannels for all-solid-state batteries. Energy Environ. Sci. 11, 185-201 (2018). https://doi.org/10.1039/C7EE02723K

[65] Pang Y. *et al*. Additive Manufacturing of Batteries. Adv. Funct. Mater. 30, 1-22 (2020). https://doi.org/10.1002/adfm.201906244

[66] Venugopal, G., Moore, J., Howard, J. & Pendalwar, S. Characterization of microporous separators for lithium-ion batteries. J. Power Sources 77, 34-41 (1999). https://doi.org/10.1016/S0378-7753(98)00168-2

[67] Blake AJ. *et al*. 3D printable ceramic-polymer electrolytes for flexible high-performance Li-ion batteries with enhanced thermal stability. Adv. Energy Mater. 7, 1-10 (2017). https://doi.org/10.1002/aenm.201602920

[68] Emanuel M. Sachs, Somerville; John S. Haggerty, Lincoln; Michael J. Cima, L. P. A. W. Three-dimensional printing techniques. US Patent US 5,204,055 45A, 14 (1993).

[69] Ziaee M, Tridas EM & Crane NB. Binder-jet printing of fine stainless steel powder with varied final density. JOM 69, 592-596 (2017). https://doi.org/10.1007/s11837-016-2177-6

[70] Lu SL, Meenashisundaram GK, Wang P, Nai SML & Wei J. The combined influence of elevated pre-sintering and subsequent bronze infiltration on the microstructures and mechanical properties of 420 stainless steel additively manufactured via binder jet printing. Addit. Manuf. 34, 101266 (2020). https://doi.org/10.1016/j.addma.2020.101266

[71] Do T. *et al*. Additively Manufactured Full-Density Stainless Steel 316L With Binder Jet Printing in Proceedings of the ASME 2018 International Manufacturing Science and Engineering Conference MSEC2018 1-10 (2018). https://doi.org/10.1115/MSEC2018-6681

[72] Upadhyay RK & Kumar A. Scratch and wear resistance of additive manufactured 316L stainless steel sample fabricated by laser powder bed fusion technique. Wear 458-459, 203437 (2020). https://doi.org/10.1016/j.wear.2020.203437

[73] Li M, Zhang X, Chen WY & Byun TS. Creep behavior of 316 L stainless steel manufactured by laser powder bed fusion. J. Nucl. Mater. 548, 152847 (2021). https://doi.org/10.1016/j.jnucmat.2021.152847

[74] Murkute P, Pasebani S & Isgor OB. Production of corrosion-resistant 316L stainless steel clads on carbon steel using powder bed fusion-selective laser melting. J. Mater. Process. Technol. 273, 116243 (2019). https://doi.org/10.1016/j.jmatprotec.2019.05.024

[75] Sutton AT, Kriewall CS, Karnati S, Leu MC & Newkirk JW. Characterization of AISI 304L stainless steel powder recycled in the laser powder-bed fusion process. Addit. Manuf. 32, 100981 (2020). https://doi.org/10.1016/j.addma.2019.100981

[76] Zhong W, Li F, Zhang Z, Song L & Li Z. Short fiber reinforced composites for fused deposition modeling. Mater. Sci. Eng. A 301, 125-130 (2001). https://doi.org/10.1016/S0921-5093(00)01810-4

[77] Weng Z, Wang J, Senthil T & Wu L. Mechanical and thermal properties of ABS/montmorillonite nanocomposites for fused deposition modeling 3D printing. Mater. Des. 102, 276-283 (2016). https://doi.org/10.1016/j.matdes.2016.04.045

[78] Vicente CMS, Martins TS, Leite M, Ribeiro A & Reis L. Influence of fused deposition modeling parameters on the mechanical properties of ABS parts. Polym. Adv. Technol. 31, 501-507 (2020). https://doi.org/10.1002/pat.4787

[79] Wang L, Sanders JE, Gardner DJ & Han Y. Effect of fused deposition modeling process parameters on the mechanical properties of a filled polypropylene. Prog. Addit. Manuf. 3, 205-214 (2018). https://doi.org/10.1007/s40964-018-0053-3

[80] Reyes C. *et al*. Three-dimensional printing of a complete lithium ion battery with fused filament fabrication. ACS Appl. Energy Mater. 1, 5268-5279 (2018). https://doi.org/10.1021/acsaem.8b00885

[81] Nicole Kareta. Blackstone Develops 3D Printed Solid-State Batteries. Spotlight Metal - the network for light metal casting (2020). https://www.spotlightmetal.com/blackstone-develops-3d-printed-solid-state-batteries-a-978392/

[82] Ren J. *et al*. Elastic and wearable wire-shaped lithium-ion battery with high electrochemical performance. Angew. Chemie - Int. Ed. 53, 7864-7869 (2014). https://doi.org/10.1002/anie.201402388

[83] Deiner LJ, Bezerra CAG, Howell TG & Powell AS. Digital Printing of Solid-State Lithium-Ion Batteries. Adv. Eng. Mater. 21, 1-18 (2019). https://doi.org/10.1002/adem.201900737

[84] Rayung M. *et al*. Bio-based polymer electrolytes for electrochemical devices: Insight into the ionic conductivity performance. Materials (Basel). 13(4), 838, (2020). https://doi.org/10.3390/ma13040838

[85] Shemonsky L. Smart buildings, smarter industry. ifm efector 3-4 (2015).

Received on 05-07-2021 Accepted on 16-08-2021 Published on 07-09-2021

DOI: https://doi.org/10.31875/2410-4701.2021.08.7